J. Integr. Sci. Technol. 2023, 11(4), 558 Article

Journal of Integrated
SCIENCE & TECHNOLOGY

Development and optimization of *Andrographis paniculata* extract-loaded phytosomes using Box-Behnken design approach

Amarpal Singh,[1] Sandeep Arora,[2]* Thakur Gurjeet Singh[1]

[1]*Chitkara College of Pharmacy, Chitkara University, Punjab, India.* [2]*Amity Institute of Pharmacy, Amity University, Noida, Uttar Pradesh, India*

Received on: 02-Dec-2022, Accepted and Published on: 24-Jan-2023

ABSTRACT

In current research, *Andrographis paniculata* extracts loaded phytosomes were successfully synthesized by thin-film hydration technique using soy lecithin and cholesterol and optimized by Box-Behnken design. The quadratic equation for % entrapment efficiency was found Y1 = 69.22 + 15.23 X1 – 0.7775 X2 – 2.65 X3 – 1.025 X1X2 + 2.41 X1X3 – 1.56 X2X3 + 6.95 $X1^2$ – 7.21 $X2^2$ – 5.52 $X3^2$ and for percentage yield was found Y2 = 70.43 + 13.86 X1 – 0.2025 X2 – 0.6962 X3 – 0.2425 X1X2 + 1.86 X1X3 – 1.43 X2X3 + 6.47 $X1^2$ – 6.75 $X2^2$ – 3.83 $X3^2$. These equations demonstrated that lipid: drug (X1) have significant effect on entrapment efficiency (Y1) and yield (Y2). The values of independent variables for optimized phytosomes were lipid: extract (X1 = 1: 1 w/w), temperature (X2 = 43°C) and time (X3 = 2.15 hours) which have D-value of 0.929. The % bias between actual and predicted values of Y1 and Y2 was 1.25% and 2.36%, respectively which concluded authenticity of design model.

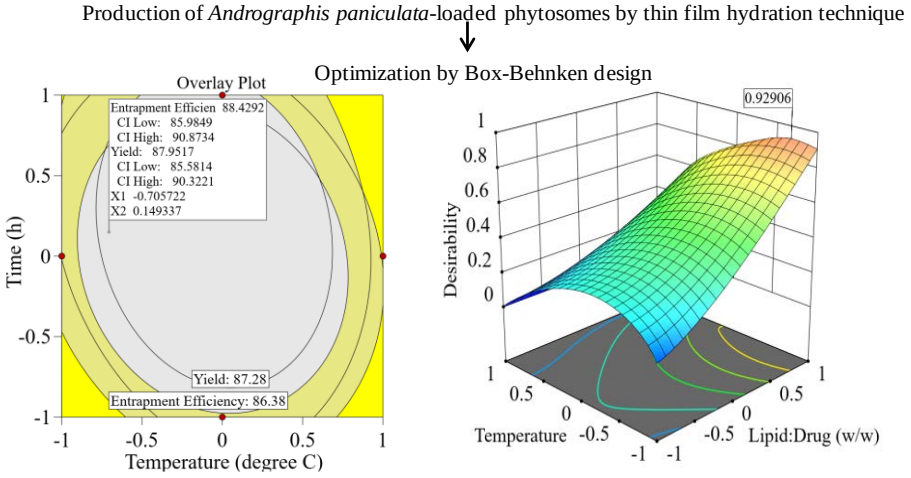

Keywords: Andrographis paniculata, Box-Behnken Design, Phytosomes, Thin-Film Hydration, Entrapment Efficiency

INTRODUCTION

Liver damage and malfunction starts with small incidence of damage to hepatocytes by different factors including viral, bacterial or other infections, alcoholic, drug induced or fatty damage leading to inflammatory changes causing hepatitis, which may start as acute change to chronic hepatitis, gradually accumulating fibrous tissue around necrotized areas and advancing to fibrosis and steatosis which may gradually become irreversible as cirrhosis.[1] All liver changes are well manifested by changes in hepatic enzyme levels, serum bilirubin and biliverdin and antioxidant capacity. Liver has a capacity to regenerate until the condition changes to fibrosis and cirrhosis, when bile duct and hepatic duct structures are damaged creating changes in serum biliary enzyme content which gets evident as jaundice. Various synthetic medicinal agents have been tried, but a comprehensive herbal have patient compliant remains the need of the hour.[2] Phytosome technology can be explored for incorporation of standardized plant extracts or water-insoluble phytoconstituents into phospholipids to produce lipid compatible molecular complexes which improves their absorption and bioavailability.[3] Numerous plant extracts and phytoconstituents have been reported for hepatoprotectuve activity.[4–6] This has been observed that phytoconstituents act in synergism, and so it is relevant that a combination formulation can be formulated and screened for getting the best therapeutic alternative.[7,8]

In this research, *Andrographis paniculata*-loaded phytsomes were synthesized through thin film hydration technique using soy lecithin and cholesterol and formulation optimization was executed by Box-Behnken design. The objective of this research was to

*Corresponding Author: Dr. Sandeep Arora, Amity institute of Pharmacy, Amity University, Noida, Uttar Pradesh, India
Email: sand_orbbd@rediffmail.com

Cite as: *J. Integr. Sci. Technol., 2023, 11(4), 558.*
URN:NBN:sciencein.jist.2023.v11.558

 ISSN: 2321-4635
http://pubs.thesciencein.org/jist

examine influence of factors on percentage entrapment efficiency and percentage yield of extract-loaded phytosomes. The statistical and diagnostic analysis of dependent variables was done to inspect model fit and to confirm reliability of model, respectively. The optimized extract-loaded phytosomes was explored by Design-Expert software and model validation was executed by check point analysis.

MATERIALS AND METHODS

Andrographis paniculata extract was procured from NJP Healthcare Pvt. Ltd. Gujarat. Soy lecithin and cholesterol were procured from Loba Chemicals Private Limited, Mumbai, India. All other ingredients employed were of analytical grade.

Experimental design

Three-factor Box-Behnken design was used as experimental design layout for manufacturing of phytosomes. Independent and dependent parameters investigated during this research have been depicted in Table 1.[9–13]

Table 1. Independent and dependent variables studied during synthesis of extract-loaded phytosomes

Independent variables	Levels of variables		
	-1	0	+1
Lipid: Extract (w/w) (X1)	0.5:1	1:1	1.5:1
Temperature (°C) (X2)	40	50	60
Time (hrs) (X3)	1	2	3
Dependent variables			**Constraint**
Entrapment Efficiency (% w/w) (Y1)			Maximize
Yield (% w/w) (Y2)			Maximize

Production of extract-loaded phytosomes

The phytosomes were synthesized according to previously described procedure.[14–17] Extract and soy lecithin in different ratios were transferred into round bottom flask and cholesterol was mixed to above mixture which was subsequently refluxed with 20 ml dichloromethane at specific temperatures for various time intervals (Table 2). The mixture was evaporated off under vacuum to produce thin film which was hydrated with 50 mL phosphate buffer having pH 7.4. The dispersion was homogenized using probe sonicator (Ultrasonic probe sonicator, PCI analytics) at 230 voltage and 50 Hz AC current at 20 seconds, filtered using membrane filtration using 0.45 µm filter and transferred into glass vial for storage at room temperature.

Evaluation of response variables of extract-loaded phytosomes

The percentage entrapment efficiency of phytosomes was evaluated in terms of andrographolides contents within phytosomes. The phytosomes were subjected to ultracentrifuge and subsequently supernatants were kept aside for twenty minutes and analysed using UV-visible spectrophotometer at 494 nm. The percentage entrapment efficiency was determined using equation 1.[18,19]

$$\% \text{ Entrapment efficiency} = [(TAC-DAC)/TAC]*100 \quad \text{Eq. 1}$$

Table 2. Box-Behnken design layout with experimental values of response variables of extract-loaded phytosomes (Batch 1-15)

Batch	Independent variables			Dependent variables	
	X1	X2	X3	Y1	Y2
1	-1	-1	0	53.22	56.65
2	1	-1	0	86.38	85.23
3	-1	1	0	51.75	55.56
4	1	1	0	84.5	83.17
5	-1	0	-1	61.59	62.57
6	1	0	-1	84.73	86.21
7	-1	0	1	51.75	56.22
8	1	0	1	84.51	87.28
9	0	-1	-1	58.43	58.11
10	0	1	-1	60.11	61.73
11	0	-1	1	55.98	60.82
12	0	1	1	51.43	58.73
13	0	0	0	69.1	72.16
14	0	0	0	70.2	68.35
15	0	0	0	68.35	70.78

X1: Lipid: Drug (w/w); X2: Temperature (°C); X3: Time (hrs); Y1: EE (% w/w); Y2: Yield (% w/w)

Where, TAC and DAC are theoretical and detected andrographolides content, respectively. Percent yield (Y2) was determined as percentage weight fraction of phytosomes with initial total weight of extracts, soy lecithin and cholesterol (Eq. 2).[20–22]

$$\% \text{ Yield} = [W1/W2]*100 \quad \text{Eq. 2}$$

Where, 'W1' is final weight of phytosomes collcted and 'W2' is initial weight of extract, soy lecithin and cholesterol.

Analysis of response variables by Design-Expert

The selection of appropriate model for response variables analysis was performed on the basis of sequential *p*-values and lack-of-fit *p*-values of linear, 2-FI (2-factors-interaction), quadratic and cubic model.[23–25] Statistical analysis was executed by analysis of variance was executed to determine *p*-value for independent parameters. The diagnostic analysis was executed to check for outliers in design model. The contour and response surface plots were obtained which demonstrated graphical view of independent *versus* response variables.[26–29]

Optimization and validation of extract-loaded phytosomes

Optimal values of parameters for production of optimized batch of phytosome with highest overall desirability function (D-value) were obtained through analysis.[30,31] The new check point batch of phytosome was synthesized to validate optimization strategy by estimating percentage bias using Eq. (3).

$$\% \text{ Bias} = [PV-EV/PV]*100 \quad \text{Eq. 3}$$

Where, PY is predicted value and EV is experimental value.

RESULTS AND DISCUSSION

Analysis of entrapment efficiency (% w/w) (Y1)

The quadratic model was selected for entrapment efficiency (Y1) since this was found that quadratic model has maximum R^2 value of 0.9942, insignificant lack of fit value of 0.1745 and sequential *p*-value of 0.0002 (Table 3). Figure 1 demonstrated

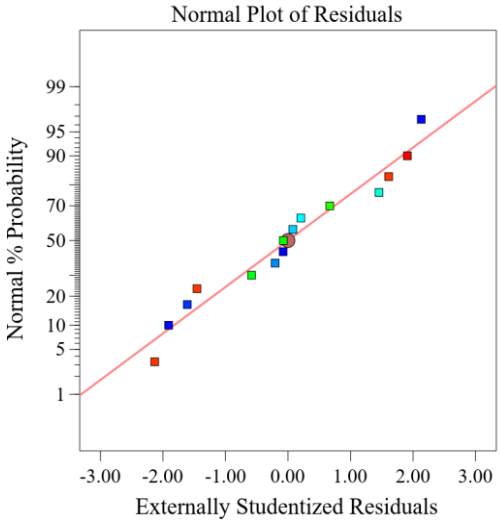

Figure 1. Normal probability plot of residuals for percentage entrapment efficiency

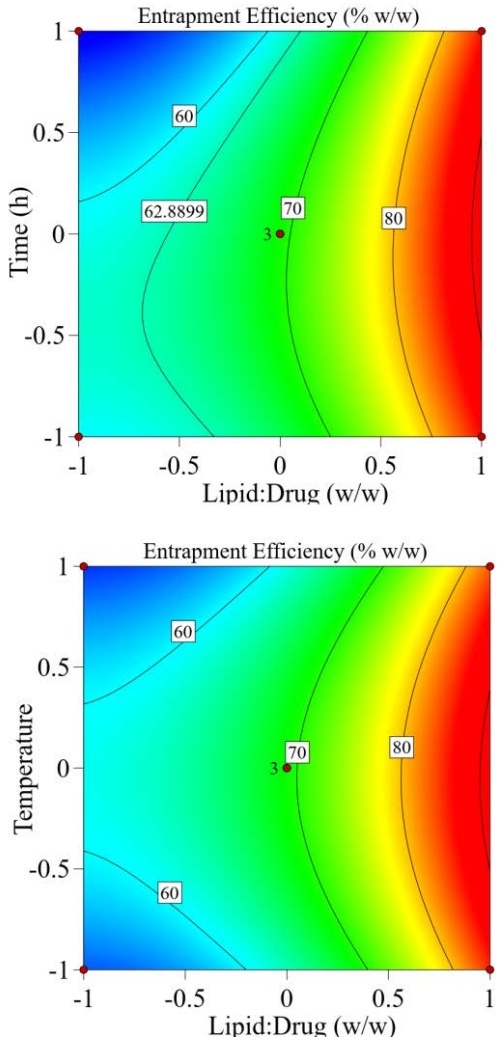

Figure 2. Illustration of effect of independent variables over percentage entrapment efficiency using two-dimensional contour plots

normal probability plot of residuals for percentage entrapment efficiency which revealed normality of data. Quadratic equation for percentage entrapment efficiency (Y1) developed by multiple regression analysis has been depicted below:

% Entrapment efficiency (Y1) = 69.22 + 15.23 X1 – 0.7775 X2 – 2.65 X3 – 1.025 X1X2 + 2.41 X1X3 – 1.56 X2X3 + 6.95 $X1^2$ – 7.21 $X2^2$ – 5.52 $X3^2$ Eq. (4)

The negative value of coefficient for X2 and X3 revealed their antagonistic action while the positive value of coefficient for X1 demonstrated their synergistic influence on Y1 of phytosomes.[32–35] The *p*-value for X1, X3, $X1^2$, $X2^2$ and $X3^2$ was less than 0.05 (Table 4) which illustrated that lipid: extract (X1) and time (X3) significantly affected entrapment efficiency (Y1) as indicated through response surface graphs (Figure 2 and 3).[19–24,36] The increase in percentage entrapment efficiency with increase in lipid: extract from 0.25:1 to 1:1 might be due to increase in amount of lipid which provide more space to accommodate extract.[11,37,38]

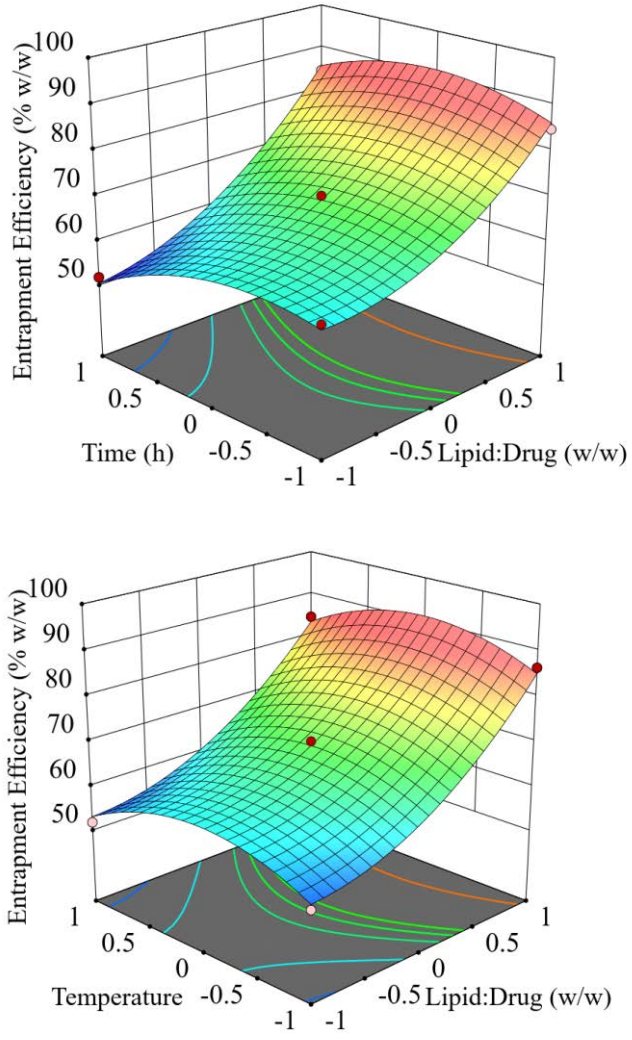

Figure 3. Illustration of effect of independent variables over percentage entrapment efficiency using three-dimensional response surface plots

Table 1. Fit summary and lack of fit statistics of Y1 and Y2

Source	Parameter	R^2	Lack of Fit *p*-value	Sequential *p*-value
Linear	Y1	0.7734	0.0138	0.0007
	Y2	0.7780	0.0739	0.0006
2FI	Y1	0.7866	0.0098	0.9164
	Y2	0.7892	0.0525	0.9323
Quadratic	Y1	0.9942	0.1745	0.0002
	Y2	0.9932	0.6965	0.0004
Cubic	Y1	0.9993	-	0.1745
	Y2	0.9962	-	0.6965

Table 2. Analysis of variance of percentage entrapment efficiency

Source	Sum of Squares	Df	Mean Square	F-value	p-value
Model	2462.68	9	273.63	94.82	< 0.0001
X_1	1854.71	1	1854.71	642.72	< 0.0001
X_2	4.84	1	4.84	1.68	0.2520
X_3	56.13	1	56.13	19.45	0.0070
X_1X_2	0.0420	1	0.0420	0.0146	0.9086
X_1X_3	23.14	1	23.14	8.02	0.0366
X_2X_3	9.70	1	9.70	3.36	0.1262
X_1^2	178.43	1	178.43	61.83	0.0005
X_2^2	191.72	1	191.72	66.44	0.0005
X_3^2	112.64	1	112.64	39.03	0.0015
Lack of fit	12.70	3	4.23	4.89	0.1745

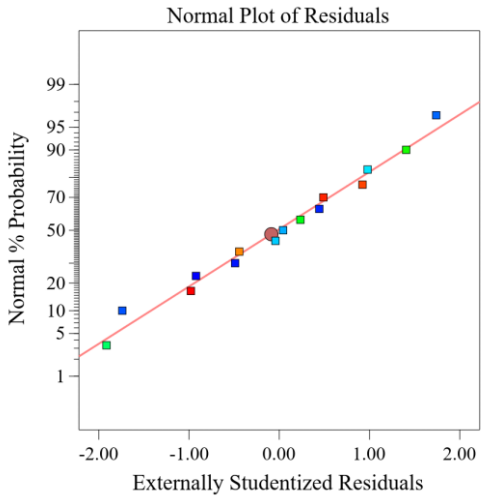

Figure 4. Normal probability plot of residuals for percentage entrapment efficiency

Analysis of yield (% w/w) (Y2)

The quadratic model was chosen for % yield (Y2) due to highest R^2 of 0.9932, insignificant ($p > 0.05$) lack of fit of 0.6965 and sequential *p*-value of 0.0004 (Table 3). Figure 4 revealed normal probability plot of residuals for percentage yield which revealed normality of percentage yield values. Quadratic equation for percentage yield (Y2) created by regression analysis as shown in Eq. 5.

$$\% \text{ Yield (Y2)} = 70.43 + 13.86\ X1 - 0.2025\ X2 - 0.6962\ X3 - 0.2425\ X1X2 + 1.86\ X1X3 - 1.43\ X2X3 + 6.47\ X1^2 - 6.75\ X2^2 - 3.83\ X3^2 \quad \text{Eq. (5)}$$

Equation 5 depicted that X1 produced synergistic effect on percentage yield while X2 and X3 caused antagonistic effect on % yield of phytosomes. X1, $X1^2$, $X2^2$ and $X3^2$ have *p*-value less than 0.05 which showed their significant effect on Y2 (Table 3).[21–23] The percentage yield rapidly increased with increase in lipid: extract due to presence of greater amount of lipids (Figure 5 and 6).[39–41]

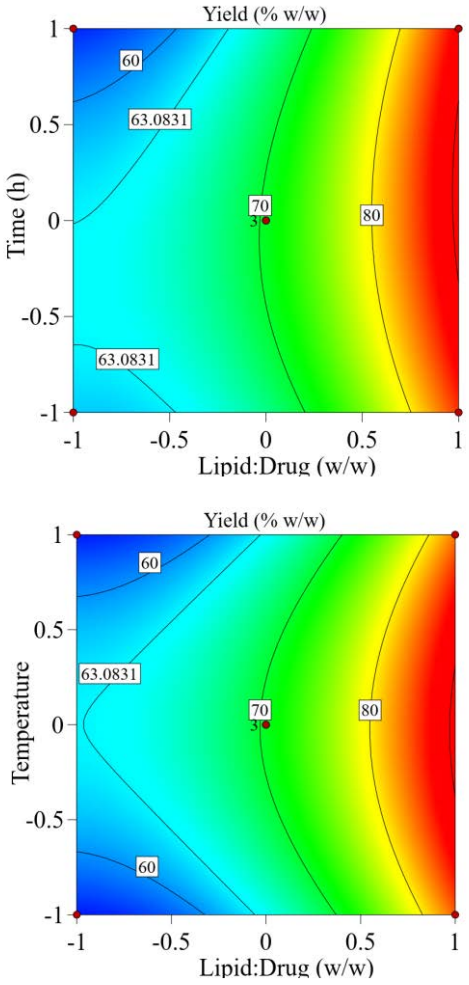

Figure 5. Illustration of effect of independent variables over percentage yield using two-dimensional contour plots

Optimization and validation of extract-loaded phytosomes

The desirability function (D-value) was investigated by Design-Expert to investigate optimized phytosome with pre-determined constraints of maximizing the percentage entrapment efficiency and percentage yield. The factors values for optimized phytosome were lipid: extract (X1 = 1: 1 w/w), temperature (X2 = 43°C) and time (X3 = 2.15 hours). D-value for optimized phytosomes was found 0.929 having predicted Y1 and Y2 of 88.43% and 87.95%, respectively (Figure 7). Ramp plots (Figure 8) and overlay plot (Figure 9) demonstrated optimized values of factors and response variables of optimized phytosome.[32,42,43] Actual values of Y1 and

Y2 for check point batch were found 87.32% and 85.87%, respectively. The percentage bias for Y1 and Y2 were 1.25% and 2.36%, respectively which validated the design model.

Table 3. Analysis of variance of percentage yield

Source	Sum of Squares	Df	Mean Square	F-value	p-value
Model	1967.50	9	218.61	80.55	< 0.0001
X_1	1537.07	1	1537.07	566.37	< 0.0001
X_2	0.3280	1	0.3280	0.1209	0.7422
X_3	3.88	1	3.88	1.43	0.2855
X_1X_2	0.2352	1	0.2352	0.0867	0.7803
X_1X_3	13.76	1	13.76	5.07	0.0741
X_2X_3	8.15	1	8.15	3.00	0.1436
X_1^2	154.68	1	154.68	57.00	0.0006
X_2^2	168.23	1	168.23	61.99	0.0005
X_3^2	54.23	1	54.23	19.98	0.0066
Lack of fit	6.13	3	2.04	0.5490	0.6965

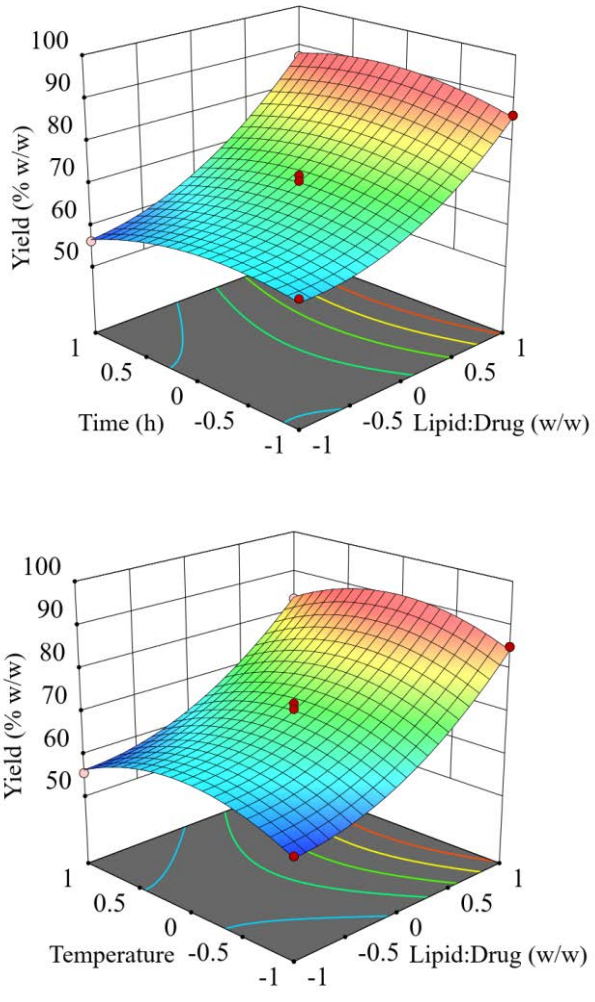

Figure 6. Depiction of effect of independent variables over percentage yield using three-dimensional response surface plots

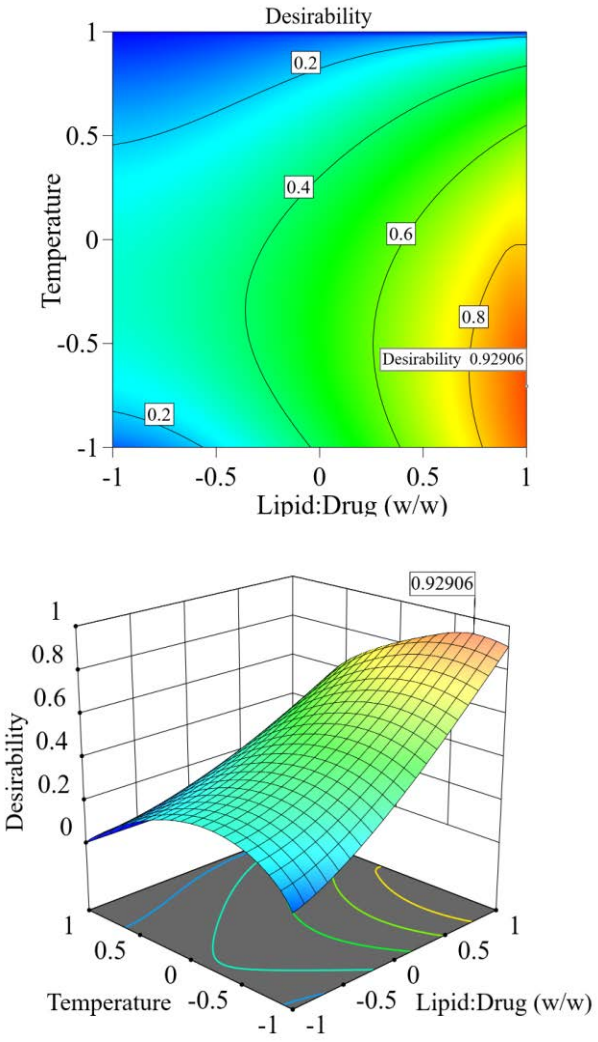

Figure 7. Contour and response surface plots depicting desirability function of optimized phytosome

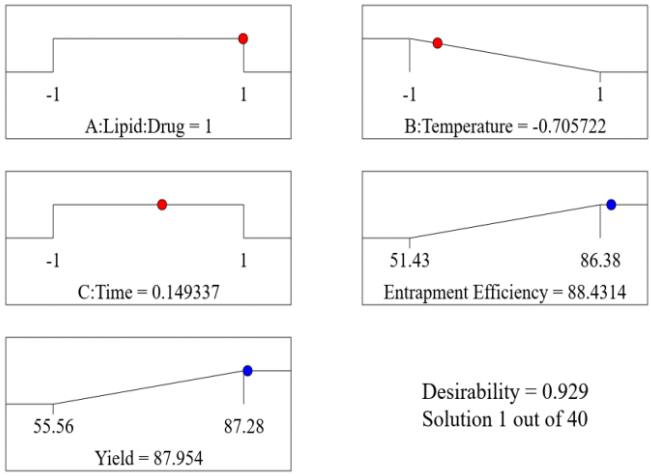

Figure 8. Ramp plots depicting optimized values of independent and dependent variables and desirability values of optimized phytosome

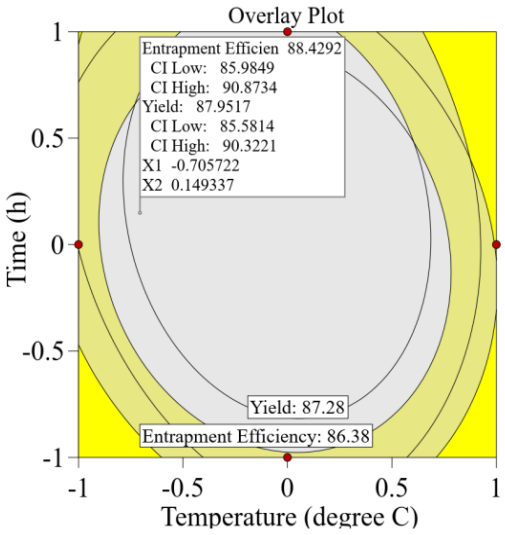

Figure 9. Overlay plot depicting predicted optimized values of independent and dependent variables (in square box) of optimized phytosome

CONCLUSIONS

In this research, *Andrographis paniculata* extracts loaded phytosomes were successfully synthesized by thin-film hydration procedure using soy lecithin and cholesterol. Box-Behnken design was used as optimization tool to explore optimized phytosomes. The research concluded that values of factors for optimized phytosomes were lipid: extract (X1 = 1: 1 w/w), temperature (X2 = 43ºC) and time (X3 = 2.15 hours) having D-value 0.929. Furthermore, the percentage bias between actual and predicted values of Y1 and Y2 was 1.25% and 2.36%, respectively which concluded autheticity of design model.

ACKNOWLEDGMENTS

The authors wish to thank Chitkara College of Pharmacy, Chitkara University, Punjab, and Amity University, Noida, India for providing infrastructural support for this research study.

CONFLICTS OF INTEREST

The authors do not have any conflicts of interest.

REFERENCES

1. J. Patterson, H.S. Hussey, S. Silal, et al. Systematic review of the global epidemiology of viral-induced acute liver failure. *BMJ Open* **2020**, 10 (7), e037473.
2. Z. Ma, B. Zhang, Y. Fan, et al. Traditional Chinese medicine combined with hepatic targeted drug delivery systems: a new strategy for the treatment of liver diseases. *Biomed. Pharmacother.* **2019**, 117, 109128.
3. N.S. Chauhan, R. Gowtham, B. Gopalkrishna. Phytosomes: a potential phyto-phospholipid carriers for herbal drug delivery. *J Pharm Res* **2009**, 2 (7), 1267–1270.
4. S. Selim, N. Akter, S.I. Nayan, et al. Flacourtia indica fruit extract modulated antioxidant gene expression, prevented oxidative stress and ameliorated kidney dysfunction in isoprenaline administered rats. *Biochem. Biophys. Reports* **2021**, 26, 101012.
5. M.A. Dkhil, S. Al-Quraishy, A.M. Aref, et al. The potential role of Azadirachta indica treatment on cisplatin-induced hepatotoxicity and oxidative stress in female rats. *Oxid. Med. Cell. Longev.* **2013**, 2013.
6. C.-C. Lin, D.-E. Shieh, M.-H. Yen. Hepatoprotective effect of the fractions of Ban-zhi-lian on experimental liver injuries in rats. *J. Ethnopharmacol.* **1997**, 56 (3), 193–200.
7. X. Zhou, S.W. Seto, D. Chang, et al. Synergistic effects of Chinese herbal medicine: a comprehensive review of methodology and current research. *Front. Pharmacol.* **2016**, 7, 201.
8. N. Murugesan, C. Damodaran, S. Krishnamoorthy, M. Raja. In-vitro evaluation of synergism in antioxidant efficiency of Quercetin and Resveratrol. *Chem. Biol. Lett.* **2023**, 10 (2), 534..
9. S. Sukhbir, S. Yashpal, A. Sandeep. Development and statistical optimization of nefopam hydrochloride loaded nanospheres for neuropathic pain using Box–Behnken design. *Saudi Pharm. J.* **2016**, 24 (5).
10. S.M. Alshahrani. Optimization and Characterization of Cuscuta reflexa Extract Loaded Phytosomes by the Box-Behnken Design to Improve the Oral Bioavailability. *J. Oleo Sci.* **2022**, ess21318.
11. N.A. Alhakamy, U. A. Fahmy, S.M. Badr-Eldin, et al. Optimized icariin phytosomes exhibit enhanced cytotoxicity and apoptosis-inducing activities in ovarian cancer cells. *Pharmaceutics* **2020**, 12 (4), 346.
12. P.A. Ittadwar, P.K. Puranik. Novel umbelliferone phytosomes: development and optimization using experimental design approach and evaluation of photo-protective and antioxidant activity. *Int. J. Pharm. Pharm. Sci* **2017**, 9, 218–228.
13. S. Tanga, B. Maji. Recent trends in precision drug and gene delivery. *Appl. NanoMedicine* **2022**, 22 (2), 429.
14. O.N. El-Gazayerly, A.I.A. Makhlouf, A.M.A. Soelm, M.A. Mohmoud. Antioxidant and hepatoprotective effects of silymarin phytosomes compared to milk thistle extract in CCl4 induced hepatotoxicity in rats. *J. Microencapsul.* **2014**, 31 (1), 23–30.
15. R.K. Sari, Y.H. Prayogo, S.A. Rozan, M. Rafi, I. Wientarsih. Antioxidant Activity, Sun Protection Activity, and Phytochemical Profile of Ethanolic Extracts of Daemonorops acehensis Resin and Its Phytosomes. *Sci. Pharm.* **2022**, 90 (1), 10.
16. N. Nagpal, M. Arora, G. Swami, R. Kapoor. Designing of a phytosome dosage form with Tecomella undulata as a novel drug delivery for better utilization. *Pak. J. Pharm. Sci.* **2016**, 29 (4), 1231–1236.
17. A.I. Abd El-Fattah, M.M. Fathy, Z.Y. Ali, A.E.-R.A. El-Garawany, E.K. Mohamed. Enhanced therapeutic benefit of quercetin-loaded phytosome nanoparticles in ovariectomized rats. *Chem. Biol. Interact.* **2017**, 271, 30–38.
18. N. Sharma, S. Singh, S. Arora, J. Madan. Quality-by-design approach for development and optimization of nefopam hydrochloride loaded poly-(epsilon-caprolactone) and poly-3-hydroxybutyrate microspheres. *Int. J. Pharm. Sci. Res.* **2017**, 8 (12), 5111–5121.
19. I. Zahoor, N. Sharma, T. Behl, S. Singh. Diagnostic Analysis and Graphical Optimization of Fenoprofen Calcium-loaded Nanostructured Lipid Carriers using Design of Experiments.
20. N. Sharma, S. Singh, N. Laller, S. Arora. Application of central composite design for statistical optimization of trigonella foenum-graecum phytosome-based cream. *Res. J. Pharm. Technol.* **2020**, 13 (4).
21. N.A. Alhakamy, U.A. Fahmy, S.M.B. Eldin, et al. Scorpion Venom-Functionalized Quercetin Phytosomes for Breast Cancer Management: In Vitro Response Surface Optimization and Anticancer Activity against MCF-7 Cells. *Polymers (Basel).* **2021**, 14 (1), 93.
22. N.A. Alhakamy, G. Caruso, M.W. Al-Rabia, et al. Piceatannol-loaded bilosome-stabilized zein protein exhibits enhanced cytostatic and apoptotic activities in lung cancer cells. *Pharmaceutics* **2021**, 13 (5), 638.
23. S. Biswas, P.K. Mukherjee, A. Kar, et al. Optimized piperine–phospholipid complex with enhanced bioavailability and hepatoprotective activity. *Pharm. Dev. Technol.* **2021**, 26 (1), 69–80.
24. O.A.A. Ahmed, S.M. Badr-Eldin, G. Caruso, et al. Colon Targeted Eudragit Coated Beads Loaded with Optimized Fluvastatin-Scorpion Venom Conjugate as a Potential Approach for Colon Cancer Therapy: In Vitro Anticancer Activity and In Vivo Colon Imaging. *J. Pharm. Sci.* **2022**, 111 (12), 3304–3317.
25. A. Singh, N. Srivastava, K.S. Yadav, P. Sinha, N.P. Yadav. Preparation, optimization, characterization and bioevaluation of rosmarinic acid loaded

phytovesicles for anti-inflammatory activity. *J. Drug Deliv. Sci. Technol.* **2020**, 59, 101888.
26. S. Singh, N. Sharma, G. Kaur. Central composite designed solid dispersion for dissolution enhancement of fluvastatin sodium by kneading technique. *Ther. Deliv.* **2020**, 11 (5).
27. N. Sharma, S. Singh. Central composite designed ezetimibe solid dispersion for dissolution enhancement: Synthesis and in vitro evaluation. *Ther. Deliv.* **2019**, 10 (10).
28. S. Singh, Y. Singla, S. Arora. Statistical, diagnostic and response surface analysis of nefopam hydrochloride nanospheres using 3^5 box-behnken design. *Int. J. Pharm. Pharm. Sci.* **2015**, 7 (10).
29. P.S. Jadon, V. Gajbhiye, R.S. Jadon, K.R. Gajbhiye, N. Ganesh. Enhanced oral bioavailability of griseofulvin via niosomes. *Aaps Pharmscitech* **2009**, 10 (4), 1186–1192.
30. P.-F. Yue, Q. Zheng, B. Wu, et al. Application of Plackett-Burman design and Box-Behnken design to achieve process optimization for Geniposide submicron emulsion. *J. Dispers. Sci. Technol.* **2012**, 33 (2), 213–222.
31. P.-F. Yue, H.-L. Yuan, X.-Y. Li, M. Yang, W.-F. Zhu. Process optimization, characterization and evaluation in vivo of oxymatrine–phospholipid complex. *Int. J. Pharm.* **2010**, 387 (1–2), 139–146.
32. P. Jain, M. Taleuzzaman, C. Kala, et al. Quality by design (Qbd) assisted development of phytosomal gel of aloe vera extract for topical delivery. *J. Liposome Res.* **2021**, 31 (4), 381–388.
33. N. Kanojia, S. Singh, N. Sharma. Development of Sustained Release Eudragit Based Matrix Tablet of Fluvastatin Sodium Microspheres. *Indian J. Pharm. Sci.* **2021**, 83 (6), 1229–1242.
34. I.K. Grewal, S. Singh, S. Arora, N. Sharma. Application of central composite design for development and optimization of eflornithine hydrochloride-loaded sustained release solid lipid microparticles. *Biointerface Res. Appl. Chem* **2021**, 112, 618–637.
35. A. Kaushal, S. Arora, N. Sharma, S. Singh. Development of Bilayer Tablet Containing Saxagliptin Immediate Release and Metformin Sustained Release Using Quality by Design Approach. *Curr. Drug ther.* **2021**, 16 (2), 184–203.
36. K. Vanaja, R.H. Shobha Rani. Design of experiments: concept and applications of Plackett Burman design. *Clin. Res. Regul. Aff.* **2007**, 24 (1), 1–23.
37. J. Kaur, M.K. Anwer, A. Sartaj, et al. ZnO Nanoparticles of Rubia cordifolia Extract Formulation Developed and Optimized with QbD Application, Considering Ex Vivo Skin Permeation, Antimicrobial and Antioxidant Properties. *Molecules* **2022**, 27 (4), 1450.
38. H.M. Alkhalidi, K.M. Hosny, W.Y. Rizg. Oral gel loaded by fluconazole–sesame oil nanotransfersomes: development, optimization, and assessment of antifungal activity. *Pharmaceutics* **2020**, 13 (1), 27.
39. N.R. Rarokar, D.R. Telange, R.P. Kalsait, P.B. Khedekar. Solubility enhancement of extract of Lagenaria siceraria by development of Phospholipon® 90 H modulated phospholipid complex employing Box-Behnken design. In *Annales Pharmaceutiques Françaises*; Elsevier, **2022**.
40. D.R. Telange, S.P. Jain, A.M. Pethe, P.S. Kharkar, N.R. Rarokar. Use of combined nanocarrier system based on chitosan nanoparticles and phospholipids complex for improved delivery of ferulic acid. *Int. J. Biol. Macromol.* **2021**, 171, 288–307.
41. N. Sinha, D. Sharma, M.S. Hussain, et al. Nanoemulsion of Mentha piperita essential oil active against Mycobacterium strains. *Chem. Biol. Lett*. **2023**, 10 (1), 507..
42. E. Bhargav, K.B. Koteshwara. A Review on Development and Characterization of a Cost-effective Targeted Quality-driven Antimalarial Product with an Emphasis on Phytosomes. *Curr. Drug Targets* **2021**, 22 (15), 1772–1788.
43. V.H. Shah, A. Jobanputra. Enhanced ungual permeation of terbinafine HCl delivered through liposome-loaded nail lacquer formulation optimized by QbD approach. *AAPS PharmSciTech* **2018**, 19 (1), 213–224.